The wavelength-dependent optical properties of weakly absorbing aqueous aerosol particles

June 23, 2020

Alison Bain and Thomas C. Preston*

Department of Atmospheric and Oceanic Sciences

and Department of Chemistry,

McGill University, 805 Sherbrooke Street West, Montreal, QC, Canada H3A 0B9

Supporting Information

* Thomas C. Preston

e-mail: thomas.preston@mcgill.ca

S1 Experimental

The following solutes were used with no further purification: Sucrose (Fisher Chemical), tartaric acid (BDH Inc.), D-mannose (Sigma Aldrich), citric acid (Fisher Chemical), NaCl (ACP Chemicals Inc.), $(NH_4)_2SO_4$ (Fisher Chemical), $NaNO_3$ (Sigma Aldrich), $MgSO_4$ (Sigma Aldrich), $NaHSO_4$ (anhydrous, $>$ 95% pure Sigma Aldrich), NaBr (ACP Chemicals Inc.), KBr (Sigma Aldrich), LiCl (MP Biomedicals, LLC), KCl (ACP Chemicals Inc.), Na_2SO_4 (Fisher Chemical), $CaCl_2$ (anhydrous, Fisher Chemical), NH_4Cl (ACP Chemicals Inc.), and $MgCl_2$ (Fisher Chemical). Solutes were dissolved in deionized water to make aqueous solutions. Concentration of the solution depended on the solute but ranged from 0.5 – 2 M. 1:1 by mole $MgSO_4$:$MgCl_2$ was made using the same solutes mentioned above, with each at a concentration of 1M in deionized water. Solutions were nebulized with a medical nebulizer (Micro-Air, Omron or TurboBOY SX, PARI) and drawn into the trapping cell.

Two different optical setups were used in these experiments, optical tweezers and a dual-beam optical trap (Fig. S1). The optical setups for the optical tweezers[1] and the dual-beam optical trap[2] have both been previously reported.

The optical tweezers are formed using a $\lambda = 532$ nm laser (Laser Quantum Opus 532) that is focused into a trapping cell with a 100$\times$ oil immersion objective (Olympus PLN 100$\times$, NA = 1.25). Depending on their size, particles were trapped and held with laser powers from 5 – 30 mW. Elastic back scattering from a broadband light source (Ocean Optics HL-2000) introduced through the trapping objective is collected back through the same objective and directed towards a spectrometer (Prinston Instruments Isoplane 320) and CCD (Prinston Instruments PIXIS 100). Spectra were collected from 550 – 800 nm with a 1200 groove/mm grating in five

steps using the step & glue function in Princeton Instruments' LightField software. In this way, we are able to obtain high resolution spectra over a broad spectral range.

The dual-beam optical trap also uses a $\lambda = 532$ nm laser (Laser Quantum Opus 532) which is split along two beam paths with a polarizing beam splitter. The two beams are focus into the trapping cell with 50× long working distance objective lenses (Olympus SLMPLN50X). The two co-axial objective lenses are aligned so that they share a common focal point. Particles were trapped with 100 mW total laser power. The forward and backward Raman scattering from the trapped particle was collected through one of the trapping objectives and directed into the spectrograph (Prinston Instruments Isoplane 320) and CCD (Prinston Instruments PIXIS 100). Cavity-enhanced Raman scattering (CERS) spectra were collected over the spontaneous Raman band of water with a 1200 groove/mm grating.

The relative humidity (RH) in either of the cells is adjusted using two mass flow controllers (MKS Instruments MF-1); mixing dry and saturated nitrogen. Air flow rates through the cell were typically between 30 – 50 sccm for the optical tweezers and 100 sccm for the dual-beam optical trap. Temperature and RH were measured in the trapping cell close to the trapped particle with a sensor (SHT75 Sensirion).

After becoming trapped, the aerosol particle was allowed to come to equilibrium with its RH-controlled surroundings. Once in equilibrium, five broadband scattering or CERS spectra were collected at constant RH. The RH in the cell was then adjusted and the particle was allowed equilibrate once again. In this way, broadband scattering and CERS spectra were collected for each particle over a wide range of RHs.

Solutes that undergo efflorescence were measured until just above the efflorescence point and solutes that do not undergo efflorescence were measured down to RHs of about 20%.

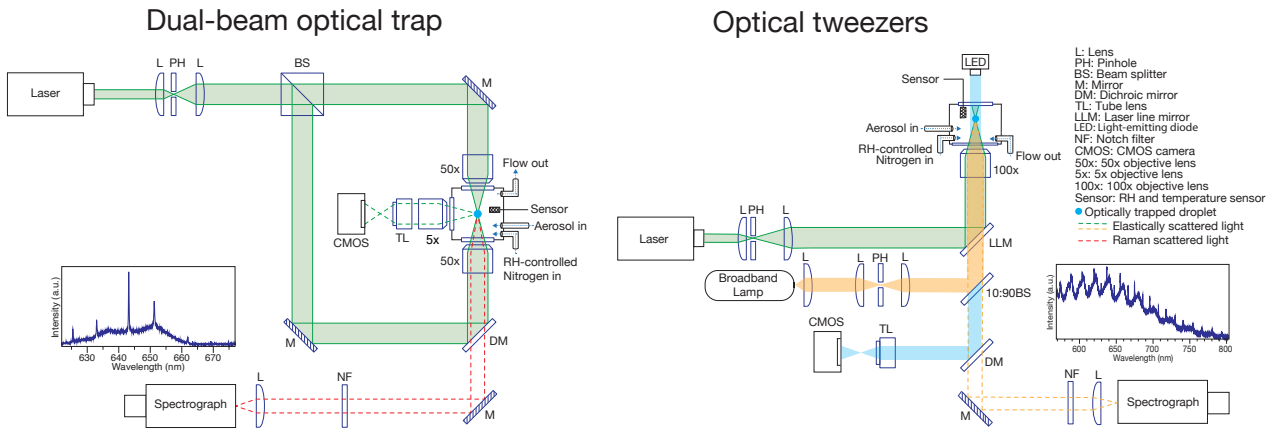

Figure S1: Optical setups for dual-beam optical trap with CERS collection and optical tweezers with broadband Mie scattering collection. Sample spectra are shown as insets.

For measurements taken in the optical tweezers, a background spectrum was taken by collecting the broadband light reflected off the coverslip after releasing the particle from the trap. This background spectrum was divided out of the scattering spectra in order to remove the background intensity. No background correction is required for CERS measurements.

S2 Data fitting

Features in the broadband scattering and CERS spectra associated with morphology dependant resonances were used to determine the refractive index (RI) of the particle using the freely available software MRFIT.[3] These resonances can be observed in exemplary CERS and broadband Mie scattering spectra inset in Fig. S1. The RI was fitted as a function of wavenumber, ν, using a Cauchy expression of the form:

$$n(\nu) = n_0 + n_1\nu^2 + n_2\nu^4, \tag{S1}$$

where $n(\nu)$ is the real part of the RI, n_0, n_1, and n_2 are found with MRFIT and $\nu = 1/\lambda$ where λ is the wavelength of light. Broadband scattering spectra were fit with all three terms while

CERS spectra were fit with only two terms.

To determine the oscillator parameters for the organic and inorganic solutes we follow the procedure outlined by Bain *et al.*[4] For an aqueous solution, the real part of the RI is

$$n(\nu) = 1 + \sum_{\alpha=1}^{J} \phi_\alpha \frac{2}{\pi} \frac{\tilde{B}_\alpha \tilde{\nu}_{0,\alpha}}{\tilde{\nu}_{0,\alpha}^2 - \nu^2} + \phi_{\mathrm{w}}(n^{(\mathrm{w})}(\nu) - 1), \tag{S2}$$

where J is the number of solutes, $n^{(\mathrm{w})}(\nu)$ is the RI of pure water (taken from Ref. 5), and ϕ_α and ϕ_w are set to be the mass fractions of solute α and water, respectively. Each solute α is characterized by a resonant wavenumber $\tilde{\nu}_{0,\alpha}$ and constant $\tilde{B}_\alpha$. By fitting experimentally measured RIs as a function of aerosol water content with Eq. S2 we can determine the effective oscillator parameters for each solute. As noted in the main text, Eq. S2 differs from the equation presented in Ref. 4 as ϕ_α and ϕ_w are mass fractions rather than relative densities. This change makes calculations much simpler as density functions are no longer required (often these functions are not known). For the aqueous systems studied here, this was found to be an excellent approximation since solution density is almost linear with solute mass fraction.

After fitting oscillator parameters for binary aqueous solutions (one solute + water, where the one solute would be, for example, NaCl), effective oscillator parameters for individual ions were subsequently determined for inorganic species by splitting each solute into contributions from anions and cations. We generated a list of equations where the RI of the solute from the solute effective oscillator parameters is equal to the RI from the ion effective oscillator parameters. As we have already found the solute effective oscillator parameters, the only unknowns were the effective oscillator parameters for the individual ions in the resulting system of equations. In our measured dataset, a number of the ions are present in more than one solute. We solved this system of equations using the `NMinimize` function in the off-the-shelf

software Mathematica and simultaneously found effective oscillator parameters for 11 ions listed in Table 1 in the main text (H^+ has no core electrons so it was assumed that $\tilde{B}_{H^+}$ and $\tilde{\nu}_{0,H^+}$ were both equal to zero).

S3 Comparing refractive index calculations

The percent difference between the effective oscillator predictions and parameterizations or models from Bain, Rafferty and Preston[4] Millard and Seaver,[6] and Cotterell *et al.*[7] for aqueous NaCl across the range of water activities shown in Fig. 2 were calculated using the following equation:

$$\text{Percent Difference} = \frac{n(\lambda)_{\text{lit}} - n(\lambda)_{\text{osc}}}{(n(\lambda)_{\text{lit}} + n(\lambda)_{\text{osc}})/2} \times 100\% \tag{S3}$$

where subscripts 'lit' and 'osc' refer to the RI from a model or parameterization from the literature and the oscillator model, respectively. The percent difference is plotted as a function of wavelength for several water activities in Fig. S2.

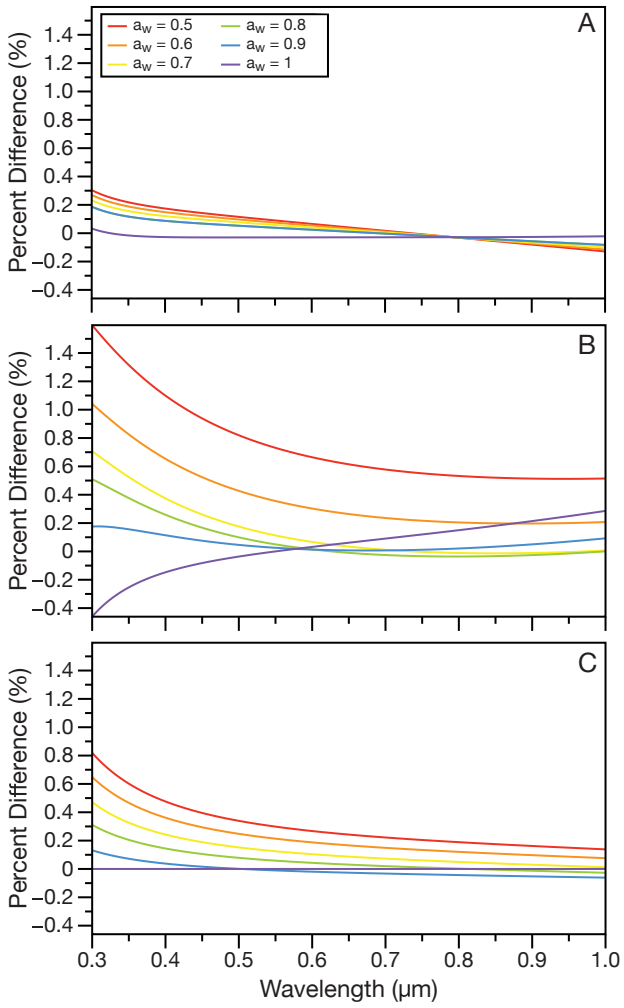

Figure S2: Percent differences between the oscillator model used here and models or parameterizations from A) Millard and Seaver[6] B) Cotterell *et al.*[7] and C) Bain, Rafferty and Preston[4] for NaCl at a range of water activities.

References

1. Lew, L. J. N., Ting, M. V. & Preston, T. C. Determining the size and refractive index of homogeneous spherical aerosol particles using Mie resonance spectroscopy. *Appl. Opt.* **57**, 4601–4609 (2018).

2. Rafferty, A. & Preston, T. C. Measuring the size and complex refractive index of an aqueous aerosol particle using electromagnetic heating and cavity-enhanced Raman scattering. *Phys. Chem. Chem. Phys.* **20**, 17038–17047 (2018).

3. Mie Resonance Fitting (MRFIT). `http://www.meteo.mcgill.ca/ tpreston/code.html`.

4. Bain, A., Rafferty, A. & Preston, T. C. The wavelength-dependent complex refractive index of hygroscopic aerosol particles and other aqueous media: An effective oscillator model. *Geophys. Res. Lett.* **46**, 10636–10645 (2019).

5. Daimon, M. & Masumura, A. Measurement of the refractive index of distilled water from the near-infrared region to the ultraviolet region. *Appl. Opt.* **46**, 3811–3820 (2007).

6. Millard, R. & Seaver, G. An index of refraction algorithm for seawater over temperature, pressure, salinity, density, and wavelength. *Deep Sea Res. Part 1 Oceanogr. Res. Pap.* **37**, 1909–1926 (1990).

7. Cotterell, M. I., Willoughby, R. E., Bzdek, B. R., Orr-Ewing, A. J. & Reid, J. P. A complete parameterisation of the relative humidity and wavelength dependence of the refractive index of hygroscopic inorganic aerosol particles. *Atmos. Chem. Phys.* **17**, 9837–9851 (2017).